

Journal of Organometallic Chemistry, 395 (1990) 279–292
 Elsevier Sequoia S.A., Lausanne
 JOM 21103

Syntheses and reactivity of *p*-substituted benzonitrile complexes derived from dicyclopentadienyl-molybdenum and -tungsten. Oxidative electrochemistry. The crystal structure of $[\text{Mo}(\eta^5\text{-C}_5\text{H}_5)_2(\text{SC}_6\text{H}_5)(p\text{-}(\text{CH}_3)_2\text{NC}_6\text{H}_4\text{CN})][\text{PF}_6]$

M.A.A.F. de C.T. Carrondo, A.R. Dias, M. Helena Garcia*, Pedro M. Matias, M. Paula Robalo

Centro de Química Estrutural, Complexo I, Instituto Superior Técnico, 1096 Lisboa Codex (Portugal)

M.L.H. Green, J. Higgins and Y.Y. Yang

Inorganic Chemistry Laboratory, South Parks Road, Oxford OX1 3QR (U.K.)

(Received February 19th, 1990)

Abstract

New cationic complexes of the type $[\text{MCp}_2(\text{SPh})(p\text{-NCC}_6\text{H}_4\text{R})][\text{PF}_6]$ ($\text{M} = \text{Mo}^{\text{IV}}$, W^{IV} ; $\text{R} = \text{H}$, CH_3 , OCH_3 , NH_2 , $\text{N}(\text{CH}_3)_2$, C_6H_5) have been prepared by chemical oxidation of the parent bithiolate in the presence of the corresponding benzonitrile derivative. Electrochemical studies, involving cyclic voltammetry carried out in dichloromethane and acetonitrile, showed a reversible or quasi-reversible oxidation for all the compounds. The molecular structure of $[\text{MoCp}_2(\text{SPh})(p\text{-NCC}_6\text{H}_4\text{N}(\text{CH}_3)_2)][\text{PF}_6]$ has been determined.

Introduction

There has been growing interest in compounds possessing donor and acceptor groups, connected by delocalised π systems, due to their demonstrated large second-order nonlinearities and potential applications on the area of integrated optics [1].

The organic compounds most used as second-order nonlinear materials are benzene derivatives bearing both an amino and a nitro or a nitrile groups, these providing the strongest donor-acceptor pairs of substituents [2]. Recent reports of relatively high second harmonic generated signals for some *para*-substituted nitriles such as *p*-MeOC₆H₄CN, *p*-H₂NC₆H₄CN [3] and *p*-MeOC₆H₄C₆H₄CN [4] prompted us to explore the possibility of enhancing their signals by coordination of the acceptor group CN to an organometallic moiety. With this in mind we have

synthesized and studied the reactions of a family of di- η^5 -cyclopentadienyl-molybdenum/tungsten nitrile derivatives and carried out a preliminary study of the optical properties of one compound of each family by the Kurtz powder technique.

Results and discussion

Chemical studies

In our previous studies of the electrochemistry of the systems $[\text{MCp}_2(\text{SR})_2]$ ($\text{M} = \text{Mo}^{\text{IV}}, \text{W}^{\text{IV}}; \text{X} = \text{Halogen, SR}$) [5] we used chemical oxidation as a convenient route to new cationic compounds derived from the MCp_2 fragment containing mixed ligands such as $[\text{MCp}_2(\text{X})\text{L}]^+$ ($\text{X} = \text{Halogen, SR}; \text{L} = \text{Nucleophile}$) [6]. The mechanism proposed for the oxidation of the parent compounds $[\text{MCp}_2(\text{X})_2]$ involves reductive elimination of X^- , followed by nucleophilic attack on the metal by the solvent or other nucleophilic species present in the solution, to give the corresponding monothiolate cations $[\text{MCp}_2(\text{X})\text{L}]^+$. We have now used this type of route, to prepare the family of new nitrile derivatives $[\text{MCp}_2(\text{SPh})(p\text{-NCC}_6\text{H}_4\text{R})][\text{PF}_6]$ ($\text{M} = \text{Mo}^{\text{IV}}, \text{W}^{\text{IV}}; \text{R} = \text{H, CH}_3, \text{OCH}_3, \text{NH}_2, \text{N}(\text{CH}_3)_2, \text{C}_6\text{H}_5$), described below.

Table 1

Analytical data for the complexes $[\text{MCp}_2\text{SR}(\text{L})][\text{PF}_6]$

Compound	Colour	Analysis (Found(calc.) (%))		
		C	H	N
$[\text{MoCp}_2(\text{SPh})(\text{NCC}_6\text{H}_5)][\text{PF}_6]$	dark-red	47.38 (47.26)	3.68 (3.45)	2.69 (2.41)
$[\text{MoCp}_2(\text{SPh})(p\text{-NCC}_6\text{H}_4\text{CH}_3)][\text{PF}_6]$	gold brown	48.42 (48.25)	3.64 (3.71)	2.16 (2.34)
$[\text{MoCp}_2(\text{SPh})(p\text{-NCC}_6\text{H}_4\text{OCH}_3)][\text{PF}_6]$	red-brown	46.85 (46.99)	3.84 (3.61)	2.13 (2.28)
$[\text{MoCp}_2(\text{SPh})(p\text{-NCC}_6\text{H}_4\text{NH}_2)][\text{PF}_6]^a$	red-brown	44.30 (46.16)	3.56 (3.53)	4.00 (4.68)
$[\text{MoCp}_2(\text{SPh})(p\text{-NCC}_6\text{H}_4\text{N}(\text{CH}_3)_2)][\text{PF}_6]$	dark-red	47.85 (47.93)	4.14 (4.02)	4.57 (4.47)
$[\text{MoCp}_2(\text{SPh})(p\text{-NCC}_6\text{H}_4\text{C}_6\text{H}_5)][\text{PF}_6]$	gold brown	51.95 (52.82)	3.94 (3.67)	2.16 (2.12)
$[\text{WCp}_2(\text{SPh})(\text{NCC}_6\text{H}_5)][\text{PF}_6]$	dark-red	41.26 (41.15)	3.10 (3.00)	1.99 (2.08)
$[\text{WCp}_2(\text{SPh})(p\text{-NCC}_6\text{H}_4\text{CH}_3)][\text{PF}_6]$	red-brown	41.59 (42.06)	3.37 (3.23)	1.82 (2.04)
$[\text{WCp}_2(\text{SPh})(p\text{-NCC}_6\text{H}_4\text{OCH}_3)][\text{PF}_6]$	red-brown	41.85 (41.10)	3.29 (3.16)	2.09 (1.99)
$[\text{WCp}_2(\text{SPh})(p\text{-NCC}_6\text{H}_4\text{NH}_2)][\text{PF}_6]$	dark-red	39.64 (40.25)	2.77 (3.08)	4.26 (4.08)
$[\text{WCp}_2(\text{SPh})(p\text{-NCC}_6\text{H}_4\text{N}(\text{CH}_3)_2)][\text{PF}_6]$	dark-red	42.27 (42.03)	3.58 (3.53)	4.08 (3.92)
$[\text{WCp}_2(\text{SPh})(p\text{-NCC}_6\text{H}_4\text{C}_6\text{H}_5)][\text{PF}_6]$	red-brick	47.44 (46.60)	3.34 (3.24)	1.83 (1.87)

^a Analysis on crude product due to its insolubility in common solvents.

The formulation of these compounds is supported by analytical data (Table 1) their ionic nature being suggested by conductivities of $75\text{--}95\text{ ohm}^{-1}\cdot\text{cm}^2\cdot\text{mol}^{-1}$ in nitromethane [7] and by the presence in the IR spectra of the 840 and 560 cm^{-1} bands characteristic of the PF_6^- anion.

Typical IR bands also confirm the presence of the cyclopentadienyl ring ($\approx 3100\text{ cm}^{-1}$) and of the coordinated nitrile, for which $\nu(\text{CN})$ stretching frequencies at $\approx 2240\text{ cm}^{-1}$ are higher than those for the free ligand for most the complexes, as observed previously for the related acetonitrile complexes [6]. This is the expected behaviour for end-on coordination to weakly back-donating metal centers. The bonding of coordinated nitriles to MCp_2L fragments has been suggested by EHMO calculation to involve a simple bond resulting from electron donation from a σ level of the nitrile to an empty orbital on the metal fragment, with π -interactions negligible [6]. The shorter Mo–N bond ($2.105(3)\text{ \AA}$) in the $[\text{MCp}_2(\text{SPh})(p\text{-NCC}_6\text{H}_4\text{N}(\text{CH}_3)_2)]^+$ (Table 4), suggesting that the metal–nitrile bond is stronger than the other molybdenum–nitrogen bonds (Table 5), probably reflects the influence of the donor group $\text{N}(\text{CH}_3)_2$ on the strength of that σ bond. These effects are in good agreement with those observed for the chemical shifts for the protons of the benzene ring in all the compounds, deshielding relative to the free ligand taking place up on coordination of the nitrile, as was expected (Table 2). However, this effect is more evident for the tungsten $p\text{-NCC}_6\text{H}_4\text{C}_6\text{H}_5$ derivative, for which, the ^1H NMR spectrum shows an AB pattern ($^3J(\text{HH}) = 7.90\text{ Hz}$) attributed to the protons of the ring adjacent to nitrile group, which for the free ligand give a sharp singlet.

Since centrosymmetry precludes second harmonic generation and crystal data showed that $[\text{MoCp}_2(\text{SPh})(p\text{-NCC}_6\text{H}_4\text{N}(\text{CH}_3)_2)]\text{PF}_6$ crystallises in the centrosymmetric space group, $P2_1/n$, some attempts were made to replace the hexafluorophosphate ion by a chiral anion. However neither attempts to bring about direct displacement of PF_6^- by an excess of a chiral anion, such as tartarate or cholicate, nor to oxidize the parent $[\text{MCp}_2(\text{SR})_2]$ with the corresponding chiral ferricinium salt were successful.

Reactions of the complexes $[\text{MCp}_2(\text{SPh})(p\text{-NCR})]\text{PF}_6$. The coordinated nitrile groups in these complexes are not susceptible to nucleophilic attack by alcohols and thiols, and the reaction with NH_3 leads to displacement of the nitrile ligand in the case of molybdenum complexes, and to formation of amidine complexes in the case of tungsten derivatives. The latter type of reaction has been reported previously for the acetonitrile derivatives $[\text{WCp}_2(\text{X})(\text{NCMe})]^+$ ($\text{X} = \text{SPh}, \text{Br}$), the amidine complexes being isolated and characterized by the usual techniques [6].

In the present work, the formulation of the amidine complexes $[\text{WCp}_2(\text{SPh})(\text{HN}=\text{C}(\text{R})\text{NH}_2)]^+$ was confirmed by IR spectroscopy after deuteration of the amino group, the appearance of N–D stretching bands in the region $2650\text{--}2450\text{ cm}^{-1}$ indicating that the NH_2 group in the amidine group is free, and can undergo H/D exchange.

Electrochemical studies

The electrochemistry of these two series of compounds $[\text{MCp}_2(\text{SPh})(p\text{-NCC}_6\text{H}_4\text{R})]\text{PF}_6$ ($\text{M} = \text{Mo}^{\text{IV}}, \text{W}^{\text{IV}}$; $\text{R} = \text{H}, \text{CH}_3, \text{OCH}_3, \text{NH}_2, \text{N}(\text{CH}_3)_2, \text{C}_6\text{H}_5$) was studied by cyclic voltammetry in dichloromethane and acetonitrile, between the limits imposed by the solvent i.e. ca. -1.5 and 1.6 V , (Table 3).

Table 2

¹H NMR spectral data

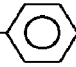
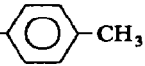
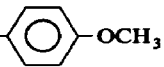
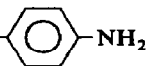
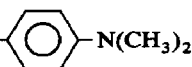
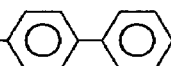
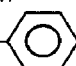
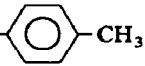
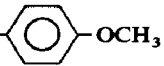
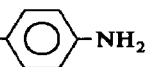
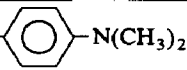
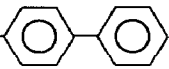
Compound [MCp ₂ (SPh)(NCR)] ⁺	τ(ppm), multiplicity, relative integrals assignment
<i>M</i> = Mo R = 	2.17 (m, 3, H ₁ , H ₃ , H ₅); 2.36 (t, 2, H ₂ , H ₄); 2.86 (d, 2, SC ₆ H ₅); 2.93 (t, 2, SC ₆ H ₅); 3.05 (t, 1, SC ₆ H ₅); 4.02 (s, 10, η ⁵ -C ₅ H ₅)
R = 	2.26 (d, 2, H ₁ , H ₄); 2.53 (d, 2, H ₂ , H ₃); 2.86 (d, 2, SC ₆ H ₅); 2.92 (t, 2, SC ₆ H ₅); 3.02 (t, 1, SC ₆ H ₅); 3.99 (s, 10, η ⁵ -C ₅ H ₅); 7.53 (s, 3, CH ₃)
R = 	2.21 (d, 2, H ₁ , H ₄); 2.86 (d, 2, H ₂ , H ₃); 2.87 (m, 4, SC ₆ H ₅); 3.02 (t, 1, SC ₆ H ₅); 4.00 (s, 10, η ⁵ -C ₅ H ₅); 6.07 (s, 3, OCH ₃)
R = 	2.55 (d, 2, H ₁ , H ₄); 2.90 (m, 4, SC ₆ H ₅); 3.02 (t, 1, SC ₆ H ₅); 3.24 (d, 2, H ₂ , H ₃); 4.05 (s, 10, η ⁵ -C ₅ H ₅); 4.40 (s, 2, NH ₂)
R = 	2.46 (d, 2, H ₁ , H ₄); 2.90 (m, 4, SC ₆ H ₅); 3.19 (t, 1, SC ₆ H ₅); 3.18 (d, 2, H ₂ , H ₃); 4.07 (s, 10, η ⁵ -C ₅ H ₅); 6.89 (s, 6, N(CH ₃) ₂)
R = 	2.06 (s, 4, H ₁ , H ₂ , H ₈ , H ₉); 2.26 (d, 2, H ₃ , H ₇); 2.49 (m, 3, H ₄ , H ₅ , H ₆); 2.85 (d, 2, SC ₆ H ₅); 2.92 (t, 2, SC ₆ H ₅); 3.02 (t, 1, SC ₆ H ₅); 3.96 (s, 10, η ⁵ -C ₅ H ₅)
<i>M</i> = W R = 	2.18 (m, 3, H ₁ , H ₃ , H ₅); 2.32 (t, 2, H ₂ , H ₄); 2.77 (d, 2, SC ₆ H ₅); 2.89 (t, 2, SC ₆ H ₅); 3.03 (t, 1, SC ₆ H ₅); 4.02 (s, 10, η ⁵ -C ₅ H ₅)
R = 	2.28 (d, 2, H ₁ , H ₄); 2.51 (d, 2, H ₂ , H ₃); 2.77 (d, 2, SC ₆ H ₅); 2.89 (t, 2, SC ₆ H ₅); 3.03 (t, 1, SC ₆ H ₅); 4.03 (s, 10, η ⁵ -C ₅ H ₅); 7.50 (s, 3, CH ₃)
R = 	2.24 (d, 2, H ₁ , H ₄); 2.82 (d, 2, H ₂ , H ₃); 2.75 (d, 2, SC ₆ H ₅); 2.88 (t, 2, SC ₆ H ₅); 3.01 (t, 1, SC ₆ H ₅); 4.05 (s, 10, η ⁵ -C ₅ H ₅); 6.05 (s, 3, OCH ₃)
R = 	2.55 (d, 2, H ₁ , H ₄); 2.77 (d, 2, SC ₆ H ₅); 2.87 (t, 2, SC ₆ H ₅); 3.01 (t, 1, SC ₆ H ₅); 3.21 (d, 2, H ₂ , H ₃); 3.85 (s, 2, NH ₂); 4.10 (s, 10, η ⁵ -C ₅ H ₅)

Table 2 (continued)

Compound [MCp ₂ (SPh)(NCR)] ⁺	τ (ppm), multiplicity, relative integrals assignment
R = 	2.47 (d, 2, H ₁ ,H ₄); 2.76 (d, 2, SC ₆ H ₅); 2.87 (t, 2, SC ₆ H ₅); 3.00 (t, 1, SC ₆ H ₅); 3.16 (d, 2, H ₂ ,H ₃); 4.11 (s, 10, η^5 -C ₅ H ₅); 6.87 (s, 6, N(CH ₃) ₂)
R = 	2.07 (m, 4, H ₁ ,H ₂ ,H ₈ ,H ₉); 2.25 (d, 2, H ₃ ,H ₇); 2.48 (m, 3, H ₄ ,H ₅ ,H ₆); 2.75 (d, 2, SC ₆ H ₅); 2.88 (t, 2, SC ₆ H ₅); 3.02 (t, 1, SC ₆ H ₅); 4.00 (s, 10, η^5 -C ₅ H ₅)

A typical cyclic voltammogram is shown in Fig. 1; such a reversible or quasi-reversible redox wave in the range 0.72–0.81 V was observed for all the compounds in both solvents. The average of the anodic and cathodic peak potentials was independent of the scan speed, and the separation of the waves ΔE_p was ca. 80 mV.

A plot of i_a against the square root of the scan speed was linear over the range of those potentials, as expected for a diffusion-controlled electrode process. This wave

Table 3

Electrochemical data ^a

Compound	E_{pa} (V)	E_{pc} (V)	$E_{p/2}$ (V)	$E_{pc} - E_{pa}$ (mV)	I_c/I_a
[MoCp ₂ (SPh)(NCC ₆ H ₅)] ⁺	0.84	0.78	0.81	65	1.0
	1.38	—	—	—	—
[MoCp ₂ (SPh)(<i>p</i> -NCC ₆ H ₄ CH ₃)] ⁺	0.74	0.67	0.71	70	1.0
	1.04	0.93	0.99	110	—
[MoCp ₂ (SPh)(<i>p</i> -NCC ₆ H ₄ OCH ₃)] ⁺	0.83	0.77	0.80	60	1.0(4)
	1.36	—	—	—	—
[MoCp ₂ (SPh)(<i>p</i> -NCC ₆ H ₄ NH ₂)] ⁺	0.80	0.74	0.77	65	1.0
[MoCp ₂ (SPh)(<i>p</i> -NCC ₆ H ₄ N(CH ₃) ₂)] ⁺	0.82	0.75	0.78	70	—
	1.27	—	—	—	—
[MoCp ₂ (SPh)(<i>p</i> -NCC ₆ H ₄ C ₆ H ₅)] ⁺	0.83	0.73	0.78	100	1.0
	1.37	—	—	—	—
[WCp ₂ (SPh)(NCC ₆ H ₅)] ⁺	0.78	0.70	0.74	80	1.1
[WCp ₂ (SPh)(<i>p</i> -NCC ₆ H ₄ CH ₃)] ⁺	0.77	0.69	0.73	80	1.0(6)
	1.25	—	—	—	—
[WCp ₂ (SPh)(<i>p</i> -NCC ₆ H ₄ OCH ₃)] ⁺	0.79	0.71	0.75	80	0.9(6)
	1.31	—	—	—	—
[WCp ₂ (SPh)(<i>p</i> -NCC ₆ H ₄ NH ₂)] ⁺ ^b	—	—	—	—	—
[WCp ₂ (SPh)(<i>p</i> -NCC ₆ H ₄ N(CH ₃) ₂)] ⁺	0.70	—	—	—	—
	1.15	—	—	—	—
[WCp ₂ (SPh)(<i>p</i> -NCC ₆ H ₄ C ₆ H ₅)] ⁺	0.76	0.67	0.72	90	1.0
	1.31	—	—	—	—

^a The electrochemical studies were carried out with CH₂Cl₂ solutions containing 0.1 M Bu₄NPF₆. Potentials are referenced to a calomel electrode containing saturated KCl solution. Sweep rates of 200 mV/s were commonly used and the temperature was 20 ± 2 °C. The solute concentration was generally about 1mM. ^b Insoluble in CH₂Cl₂.

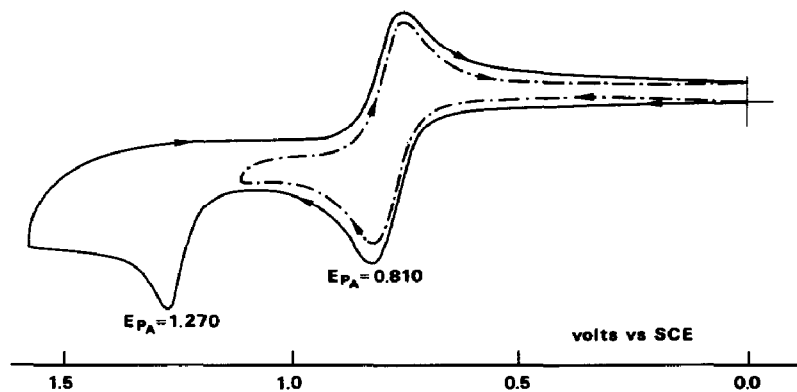


Fig. 1. Cyclic voltammogram of $[\text{MoCp}_2(\text{SPh})(p\text{-NCC}_6\text{H}_4\text{N}(\text{CH}_3)_2)][\text{PF}_6]$ in CH_2Cl_2 containing 0.1 M ${}^n\text{Bu}_4\text{NPF}_6$ (sweep rate = 200 mV/s). Initial voltage sweep indicated by dashed line.

was attributed to the oxidation $\text{M}^{\text{IV}} \rightarrow \text{M}^{\text{V}}$ by analogy with the results for the related compounds $[\text{MCp}_2\text{X}_2]$ ($\text{M} = \text{Mo}^{\text{IV}}, \text{W}^{\text{IV}}$; $\text{X} = \text{Cl}, \text{Br}, \text{I}, \text{SR}$) [5].

At higher potentials, $\approx 1.3\text{ V}$ a second irreversible anodic wave occurred, its position suggesting, in most cases, that it might correspond to an irreversible oxidation of the coordinated nitrile, leading to an immediate decomposition of the dioxidized compound. However, when the substituted nitrile ligand was $p\text{-N}(\text{CH}_3)_2\text{C}_6\text{H}_4\text{CN}$ a different behaviour was observed for both the molybdenum and tungsten derivatives. In fact, when the cyclic voltammetry was carried out in acetonitrile, in addition to the reversible anodic wave (A) at ca. 0.80 V and the irreversible anodic wave (C) at ca. 1.30 V , a third irreversible anodic wave (B) appeared at ca. 1.20 V , and became more pronounced with the time, as is shown in the cyclic voltammogram indicated by a dashed line in Fig. 2.

The characteristics of this anodic wave and its position, at the potential of the free nitrile, suggests that substitution of the coordinated nitrile by acetonitrile is taking place. The formation of the resulting acetonitrile derivative

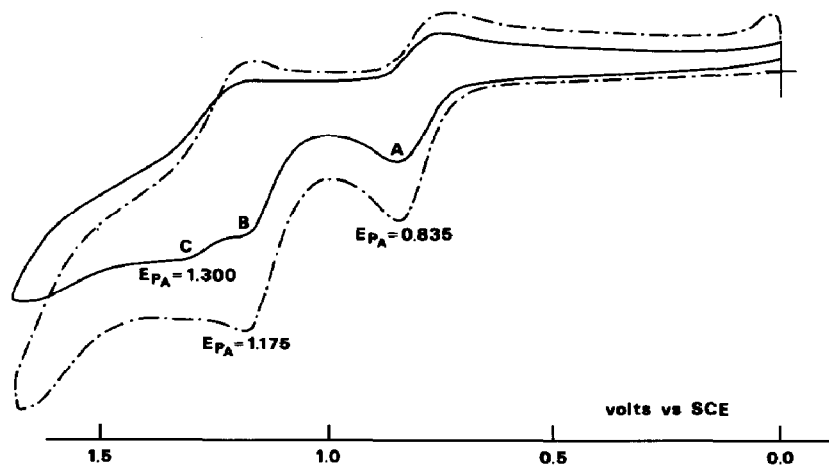


Fig. 2. Cyclic voltammogram of $[\text{MoCp}_2(\text{SPh})(p\text{-NCC}_6\text{H}_4\text{N}(\text{CH}_3)_2)][\text{PF}_6]$ in CH_3CN containing 0.1 M ${}^n\text{Bu}_4\text{NPF}_6$ (Sweep rate = 200 mV/s).

$[\text{MCp}_2(\text{SPh})(\text{NCCH}_3)]^+$ is not clearly observed since its oxidation wave [5] occurs at approximately the same potential as that for the parent compound $[\text{MCp}_2(\text{SPh})(\text{NCR})]^+$. It seems that the substitution of the coordinated nitrile NCR by acetonitrile is caused by the presence of the species $[\text{MCp}_2(\text{SPh})(\text{NCR})]^{2+}$ since acetonitrile does not displace the coordinated nitrile during the time of the electrochemical experiment if no scan potential is applied to the solution. The kinetic stability of $[\text{MoCp}_2(\text{SPh})(p\text{-NCC}_6\text{H}_4\text{N}(\text{CH}_3)_2)]^+$ relative to its acetonitrile analogue is not surprising, since structural data indicate that the Mo–N bond is stronger in the former.

Crystallographic studies

Structure of $\text{MoCp}_2(\text{SPh})(p\text{-NCC}_6\text{H}_4\text{N}(\text{CH}_3)_2)[\text{PF}_6]$. The molecular structure of $[\text{MoCp}_2(\text{SPh})(p\text{-NCC}_6\text{H}_4\text{N}(\text{CH}_3)_2)]^+$ is shown in Fig. 3 along with the atom numbering scheme. The values of selected bond lengths, bond angles, and torsion angles are given in Table 4.

The crystal structure consists of discrete $[\text{MoCp}_2(\text{SC}_6\text{H}_5)(p\text{-NCC}_6\text{H}_4\text{N}(\text{CH}_3)_2)]^+$ cations and $[\text{PF}_6]^-$ anions. The metal is coordinated to the two η^5 -cyclopentadienyl rings, the sulfur atom of the thiophenolate ligand and the nitrile nitrogen atom of the $p\text{-NCC}_6\text{H}_4\text{N}(\text{CH}_3)_2$ ligand, in a distorted tetrahedral environment. A comparison between the coordination geometry about the Mo atom is given in Table 5 for recently reported structures of $[\text{MoCp}_2\text{LL}']$ complexes containing Mo–S or Mo–N bonds. The Mo–S bond length of 2.473(1) Å is similar to those in other MoCp_2 derivatives containing S-bonded ligands. However, the Mo–N bond length of 2.105(3) Å is one of the shortest so far encountered in $[\text{MoCp}_2\text{LL}']$ complexes. The N–Mo–S angle of 79.8(1)° lies in the normal range for MoCp_2 species coordinated to two monodentate ligands, and the angle of 137.0(2)° between the Cp ring

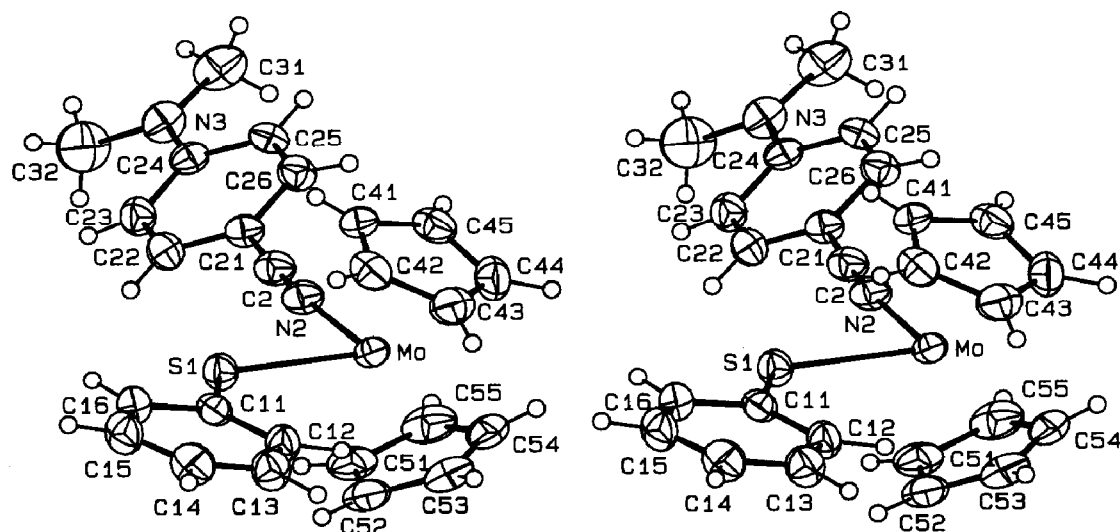


Fig. 3. ORTEP-II [31] stereoview of the $[\text{Mo}(\text{Cp})_2(\text{SC}_6\text{H}_5)(p\text{-NCC}_6\text{H}_4\text{N}(\text{CH}_3)_2)]^+$ cation, showing the atomic numbering. The thermal ellipsoids are drawn at the 50% probability level and the hydrogens are represented with a U_{iso} of 0.013 Å².

Table 4

Selected bond lengths (Å), bond angles (°) and torsion angles (°) for [MoCp₂(SPh)(*p*-NCC₆H₄N(CH₃)₂)]⁺

<i>Bond lengths</i>			
Mo–S1	2.473(1)	Mo–N2	2.105(3)
S1–C11	1.778(3)	N2–C2	1.146(5)
C11–C12	1.385(6)	C12–C13	1.379(6)
C13–C14	1.357(7)	C14–C15	1.363(7)
C15–C16	1.383(6)	C16–C11	1.393(6)
C2–C21	1.418(5)	C21–C22	1.384(6)
C22–C23	1.368(6)	C23–C24	1.404(6)
C24–C25	1.398(6)	C25–C26	1.359(6)
C26–C21	1.398(5)	C24–N3	1.355(5)
N3–C31	1.436(7)	N3–C32	1.459(8)
C41–C42	1.375(7)	C42–C43	1.375(7)
C43–C44	1.403(8)	C44–C45	1.391(7)
C45–C41	1.401(7)	C51–C52	1.405(8)
C52–C53	1.364(9)	C53–C54	1.397(8)
C54–C55	1.365(11)	C55–C51	1.412(9)
Mo–Cp(41–45) ^a	1.985(1)	Mo–Cp(51–55) ^b	1.990(1)
<i>Bond angles</i>			
S1–Mo–N2	79.8(1)	Cp–Mo–Cp ^c	137.0(2)
Mo–S1–C11	113.1(1)	Mo–N2–C2	171.7(3)
S1–C11–C12	125.1(3)	S1–C11–C16	117.9(3)
C12–C11–C16	117.0(4)	C11–C12–C13	120.5(4)
C12–C13–C14	121.8(5)	C13–C14–C15	118.9(5)
C14–C15–C16	120.4(5)	C11–C16–C15	121.3(4)
N2–C2–C21	176.9(4)	C2–C21–C22	121.8(4)
C2–C21–C26	119.8(4)	C22–C21–C26	118.4(4)
C21–C22–C23	121.3(5)	C22–C23–C24	121.0(5)
C23–C24–C25	116.9(4)	C23–C24–N3	122.4(5)
C25–C24–N3	120.7(4)	C24–C25–C26	122.2(4)
C21–C26–C25	120.2(4)	C24–N3–C31	121.7(5)
C24–N3–C32	120.2(6)	C31–N3–C32	117.3(7)
<i>Torsion angles</i>			
N2–Mo–S1–C11	–171.4(1)	S1–Mo–N2–C2	–165.6(1.5)
Mo–S1–C11–C12	–15.4(3)	Mo–S1–C11–C16	165.7(3)

^a Denotes ring centroid to C41–C45. ^b Denotes ring centroid to C51–C55. ^c Denotes angle between ring normals.

normals is also in the usual range for these kind of [MoCp₂LL'] complexes. The cyclopentadienyl rings adopt an eclipsed conformation in the crystal.

The torsion angles listed in Table 4 show that the phenyl ring is almost coplanar with Mo, S1, and N2, with $\alpha = \text{N2–Mo–S1–C11} = -171.4(1)$ and $\beta = \text{Mo–S1–C11–C12} = -15.4(3)^\circ$. This relative orientation was also observed in [MoCp₂(NH₃)(SPh)]⁺ [17], with $\alpha = -178.7(2)$ and $\beta = -6.8(5)^\circ$, and in MoCp₂(SPh)(σ -CH(CN)–CH₃) [15], with $\alpha = -156.1(1)$ and $\beta = -55.3(2)^\circ$. However, in [TiCp₂(SPh)₂]⁺ [18] the Ph rings are directed respectively above and below the plane defined by Ti and the two S atoms. EHMO calculations on the model complex M(Cp₂)(SH)₂ (M = Ti, Mo) [18] indicate that the *exo* conformation is preferred for Mo and the *endo* for Ti. It is noteworthy that a nearly *exo* conforma-

Table 5
Structural data for Mo(Cp)₂ derivatives containing ligands with nitrogen or sulfur donor atoms ^a

[MoCp ₂ -	Mo-S (Å)	Mo-N (Å)	L-Mo-L' (°)	<Mo-Cp> (Å)	Cp-Mo-Cp (°)	R	Ref.
-(NCCH ₃) ₂ ^b		2.219(7)	32.0(2)	1.954	139.2(3)	0.033	[13]
-(OC(O)NPh)		2.216(7)	32.4(2)	1.958	137.4(3)		
-(SNNC ₃ H ₄)][PF ₆]	2.500(4)	2.105(4)	61.9(1)	1.977	132.2(2)	0.055	[14]
-(S ₂ O ₃)]	2.450(2)	2.157(5)	64.9(2)	1.968	132.4(2)	0.036	[15]
-(S(t-C ₄ H ₉) ₂)]	2.501(1)		72.3(1)	1.982	133.2(3)	0.023	[16]
	2.491(1)		71.1(1)	2.020	130.4(3)	0.035	[17]
-(μ-S-t-C ₄ H ₉) ₂ NiCp]	2.510(2)		68.7(1)	1.987	128.3(5)	0.050	[18]
-(NCCH ₃)][PF ₆]		2.124(6)	81.2(1)	1.976	133.8(3)	0.057	[6]
-(SPh)σ-CH(CN)-CH ₃]	2.500(1)		77.4(1)	1.984	132.9(1)	0.026	[19]
-(S ₂ CN(C ₂ H ₅) ₂){σ-C(CN)=CH ₂ }]	2.474(1)		80.9(1)	1.984	136.1(2)	0.030	[19]
-S ₂ C(CO ₂ CH ₃)=C(CO ₂ CH ₃)] ^b	2.440(1)		77.3(1)	1.977	135.5(2)	0.038	[20]
	2.442(1)		76.8(1)	1.976	133.5(2)		
-S ₂ C ₁₀ H ₃ N ₃]	2.527(4)		81.0(4)	1.979	133.9(6)	0.059	[20]
-(NH ₃)(SPh)][PF ₆]	2.465(5)		76.4(4)	1.988	134.9(7)	0.047	[21]
-(SPh)(NCC ₂ H ₄ N(CH ₃) ₂)[PF ₆]	2.473(1)	2.105(3)	79.8(1)	1.988	137.0(2)	0.039	This work

^a Some of the data presented in this table were calculated from atomic coordinates retrieved from the database of the Cambridge Crystallographic Data Centre [12].

^b Two molecules in the asymmetric unit.

tion is still preferred when only one of the ligands has a S donor atom. Steric energy calculations for $[\text{MoCp}_2(\text{NH}_3)(\text{SPh})]^+$ [17] revealed three minima connected by a shallow valley, containing the ideal *exo* conformation; the crystal field might thus be responsible for the observed differences from the ideal conformation.

Inspection of the structural data in Table 5 and in similar tables [13,19] indicate that the MoCp_2 moiety of these bent metallocene complexes is typical and constant, while the value of the L–Mo–L' angle depends strongly on the geometry of the MoLL' fragment, there being no correlation between the two halves of the molecule, as predicted originally by Prout et al. [20]. Smaller L–Mo–L' angles are found for strained bidentate ligands that form three-membered rings as in complex 1, four-membered rings as in complexes 2 and 3, and also in $[\text{MoCp}_2(2\text{-NHNC}_5\text{H}_4)]^+[\text{PF}_6]^-$

Table 6

Fractional atomic coordinates and thermal parameters (\AA^2) for $[\text{MoCp}_2(\text{SPh})(p\text{-NCC}_6\text{H}_4\text{N}(\text{CH}_3)_2)]^+ \text{PF}_6^-$

Atom	Fractional coordinates ^b			U_{eq}^c
	x	y	z	
Mo	22361(3)	10901(1)	28600(3)	473(1)
S1	3629(1)	1787(1)	4094(1)	589(4)
N2	983(3)	1289(1)	4152(3)	60(1)
C11	5076(3)	1996(2)	3465(3)	52(1)
C12	5573(4)	1703(2)	2541(4)	63(2)
C13	6702(4)	1904(2)	2112(4)	73(2)
C14	7368(5)	2389(3)	2576(5)	78(2)
C15	6917(5)	2677(2)	3503(5)	74(2)
C16	5783(4)	2486(2)	3945(4)	64(2)
C2	214(4)	1339(2)	4803(4)	61(2)
C21	–785(3)	1383(2)	5568(3)	54(1)
C22	–514(5)	1486(2)	6743(4)	66(2)
C23	–1483(5)	1511(2)	7477(4)	65(2)
C24	–2789(4)	1433(2)	7060(3)	53(1)
C25	–3044(4)	1331(2)	5870(3)	55(2)
C26	–2081(4)	1300(2)	5141(4)	59(2)
N3	–3772(4)	1459(2)	7762(3)	69(2)
C31	–5091(6)	1327(3)	7342(7)	92(3)
C32	–3492(10)	1530(5)	9013(6)	112(4)
C41	1264(5)	1942(2)	2080(4)	64(2)
C42	2427(5)	1902(2)	1588(4)	69(2)
C43	2412(6)	1381(3)	935(4)	79(2)
C44	1209(5)	1093(2)	1000(4)	78(2)
C45	490(5)	1446(2)	1710(5)	72(2)
C51	2845(6)	346(2)	4154(5)	81(2)
C52	3912(5)	410(2)	3488(5)	76(2)
C53	3503(6)	255(2)	2375(6)	84(2)
C54	2201(6)	77(2)	2337(7)	89(3)
C55	1782(6)	129(2)	3420(7)	89(2)

^a The fractional atomic coordinates and thermal motion parameters for hydrogen atoms and the $[\text{PF}_6]^-$ anion have been deposited as supplementary Table S1. The anisotropic thermal motion parameters for $[\text{MoCp}_2(\text{SPh})(p\text{-NCC}_6\text{H}_4\text{N}(\text{CH}_3)_2)]^+[\text{PF}_6]^-$ have been deposited as supplementary Table S2. Lists of observed and calculated structure factor amplitudes have been deposited as supplementary Table S3. The Tables S1–S3 have been deposited with the Cambridge Crystallographic Data Centre. ^b Positional parameters multiplied by 10^5 for Mo and by 10^4 for other atoms. ^c U_{eq} (\AA^2) multiplied by 10^4 for Mo and S atoms, by 10^3 for other atoms.

[19], $[\text{MoCp}_2(2\text{-ONC}_5\text{H}_4)][\text{PF}_6]$ [19] and $[\text{MoCp}_2(\text{SO}_4)]$ [21], with L–Mo–L' angles of 59.8(3), 61.2(4) and 66.1(2)° respectively, or for very bulky ligands, as in complexes **5** and **6**. All the other complexes which involve no significant strain due to the ligands have an L–Mo–L' angle close to the theoretical value of 78° for d^2 bis-cyclopentadienyl complexes derived from EHMO calculations [22].

Second harmonic generation effects

Samples of randomly sized powders of the complexes $[\text{MoCp}_2(\text{SPh})(p\text{-NCC}_6\text{H}_4\text{N}(\text{CH}_3)_2)][\text{PF}_6]$ and $[\text{WCp}_2(\text{SPh})(p\text{-NCC}_6\text{H}_4\text{C}_6\text{H}_5)][\text{PF}_6]$ were tested for second harmonic generation (SHG) efficiencies, using the Kurtz powder technique [23]. Since the compounds are red, light from a Nd:YAG laser operating at 1.064 μm was Raman shifted to 1.907 μm with a high pressure hydrogen gas cell.

The molybdenum compound showed no effect. The efficiency of the tungsten complex was 0.39 terms that of the area standard. The effect observed for the tungsten compound is significant, but it also includes some luminescence.

The comparison of the SHG values observed for the uncoordinated nitrile $p\text{-NCC}_6\text{H}_4\text{N}(\text{CH}_3)_2$, which had shown a high second order hyperpolarizability [3], and for our coordinated nitrile compound seems to indicate that there is no enhancement of the nonlinear optical properties of the nitrile upon coordination to the metal center. This result can be attributed to the centrosymmetry of the crystals, since examination of the X-ray structural data suggests that there is a significant delocalization of the nitrile π electron towards the organometallic moiety, this effect being related to large values for second order hyperpolarizabilities. Comparison between the bond lengths of the aromatic nitrile ring (Table 4) shows that the bonds C22–C23 and C25–C26 are significantly shorter than the other C–C bonds in the ring. On the other hand, the bond between that ring and the carbon of the nitrile group, C2–C21, is shorter than the corresponding bond in the equivalent coordinated acetonitrile compound [6], the CN distance being the same in both compounds. All these observations, together with the shorter Mo–N distance, suggest that there is an extended conjugated π double bond system in the coordinated nitrile, which would be enhanced by the presence of the donor group $\text{N}(\text{CH}_3)_2$, the organometallic moiety playing the role of acceptor. However, it is well known that systems in which the molecules pack centrosymmetrically exhibit no SHG, and that the optimum value of this SHG is observed in non-centrosymmetric structures when the angle between molecules has a particular space-group dependent value. The disappointingly low value for the compound $[\text{WCp}_2(\text{SPh})(p\text{-NCC}_6\text{H}_4\text{C}_6\text{H}_5)][\text{PF}_6]$, which is expected to crystallise in a non-centrosymmetric space group, since a substituted biphenyl group is present as a ligand, can be attributed to poor phase matching.

Although some experiments carried out in order to replace PF_6^- by a chiral counterion were unsuccessful, further work should be done to improve the alignment of the molecular dipole in the crystal lattice, and a substantially larger SHG efficiency can then be expected.

Experimental

All experiments were carried out under N_2 by standard Schlenk tube techniques. IR spectra were measured on a Perkin-Elmer 457 spectrophotometer with KBr

pellets. ^1H NMR spectra were recorded on a Bruker CXP300 spectrometer. Micro-analysis were performed in our laboratories.

$[\text{MCp}_2\text{X}_2]$ ($\text{M} = \text{Mo}^{\text{IV}}, \text{W}^{\text{IV}}; \text{X} = \text{Cl}, \text{SC}_6\text{H}_5$) were prepared from the parent dihydrides $[\text{MCp}_2\text{H}_2]$ [24] as described previously [25,26].

Preparation of $[\text{MCp}_2(\text{SPh})(\text{NCR})][\text{PF}_6]$

All the complexes were prepared by the following typical procedure. To a suspension of $[\text{MCp}_2(\text{SPh})_2]$ (1 mmol) in 30 ml of dichloromethane containing $p\text{-N}\equiv\text{CR}$ (2 mmol), a solution of $[\text{FeCp}_2][\text{PF}_6]$ (1 mmol) in 20 ml in the same solvent was added at room temperature and the mixture was stirred for 24 h then filtered. The filtrate was evaporated to dryness and the residue was washed several times with dry ether, then recrystallized from $\text{CH}_2\text{Cl}_2/\text{Et}_2\text{O}$. Yield ca. 60–80%.

Electrochemical apparatus

The electrochemistry instrumentation consisted of a Princeton Applied Research Model 173 potentiometer, a Model 175 voltage programmer, a Model 179 digital coulometer and a Houston Instruments Omnigraph 2000 X-T recorder. Potentials were referred to a calomel electrode containing a saturated solution of potassium chloride checked relative to a $1.0 \times 10^{-3} \text{ M}$ solution of ferrocene in acetonitrile containing 0.10 M LiClO_4 , for which the ferricinium/ferrocene potential was in agreement with the literature value [27].

The working electrode was made of a 2 mm piece of platinum wire and the secondary electrode was a platinum wire coil. Cyclic voltammetry experiments were performed in a PAR polarographic cell, at room temperature, solutions used being 1 mM in solute and 0.1 M in the supporting electrolyte, tetrabutylammonium hexafluorophosphate.

The solvents acetonitrile and dichloromethane were reagent grade materials, were dried over CaH_2 and P_2O_5 and distilled just before use under argon. Solutions were degassed with dry nitrogen before each experiment and a nitrogen atmosphere was maintained over the solution during the experiments.

X-ray crystal structure of $[\text{MoCp}_2(\text{SR})(p\text{-NCC}_6\text{H}_4\text{N}(\text{CH}_3)_2)][\text{PF}_6]$

Crystal data. $[\text{C}_{25}\text{H}_{25}\text{N}_2\text{SMo}]^+[\text{PF}_6]^-$, M_r 626.45, monoclinic, space group $P2_1/n$, a 10.325(2), b 22.061(4), c 11.568(2) Å, β 94.92(1)°, V 2625.26 Å³, Z 4, D_c 1.59, $\mu(\text{Mo-K}\alpha)$ 6.80 cm⁻¹.

Data collection. X-ray data were obtained with an Enraf-Nonius CAD-4 diffractometer and graphite monochromatized $\text{Mo-K}\alpha$ radiation ($\lambda = 0.71069$ Å). Cell dimensions were determined from the measured θ -values for 25 intense reflections with $11 < \theta < 15^\circ$. The intensities of 5124 independent reflections in range $1.5 \leq \theta \leq 26^\circ$ were measured by the ω - 2θ scan mode. The data were corrected for Lorentz and polarization effects, and empirical absorption corrections were applied by use of program DIFABS [28].

Structure determination and refinement. The 3343 reflections with $F > 3\sigma(F)$ were used in the structure solution and early stages of refinement. The Mo position was located from a Patterson map and the P, F, N and C positions from subsequent difference Fourier maps. Least-squares refinement with anisotropic thermal parameters for all non-H atoms gave $R = 0.068$. A difference Fourier map at this point revealed the H atom positions and 6 additional peaks around the P atom that were

interpreted as evidence of positional disorder of the F atoms in the $[\text{PF}_6]^-$ anion. Both sets of F atom positions were then refined with anisotropic thermal parameters, and occupancies constrained to obey the known stoichiometry. Finally, the H atoms were included in the refinement with individual isotropic thermal parameters. The final refinement was carried out by minimizing $\sum w(F_o^2 - F_c^2)^2$ with $w = (\sigma^2(F_o^2) + (0.03 F_o^2)^2)^{-1}$, and converged to $R(F_o^2) = 0.045$, $R_w(F_o^2) = 0.068$, $R(F) = 0.39$ and $S = 1.21$, for 3440 reflections with $F_o^2 > \sigma(F_o^2)$ and 480 refined parameters. A final difference Fourier map contained no significant features, with $\rho_{\text{max}} = 0.25$, $\rho_{\text{min}} = -0.27$ and $\sigma(\rho) = 0.09 \text{ e}/\text{\AA}^3$, estimated from the experimental $\sigma(F_o)$ values.

Final atomic coordinates and thermal parameters are given in Table 6 for all atoms except H, F and P. The atomic coordinates and thermal parameters for H, F and P atoms, anisotropic thermal parameters for all non-hydrogen atoms, and a list of observed and final calculated structure factors are available from the authors and have been deposited as supplementary material.

The computations required to solve and refine the structure were involved use of the programs SHELXS-86 [29], SHELX76 [30] and UPALS [31]. Drawings were made with program ORTEP-II [32]. Atomic scattering values were taken from International Tables [33].

Acknowledgements

Financial support of this work was provided by Junta Nacional de Investigaç o Cient fica e Tecnol gica through Grant no. BIC 360 (to Maria Paula Robalo) and by Instituto Nacional de Investigaç o Cient fica.

References

- 1 D.J. Williams (Ed.), *Nonlinear Optical Properties of Organic and Polymeric Materials*, ACS Symposium Series 233, American Chemical Society, Washington, 1983.
- 2 D.J. Williams, *Angew. Chem., Int. Ed. Engl.*, 23 (1984) 690.
- 3 A. Dulcic and C. Sauteret, *J. Chem. Phys.*, 69 (1978) 3453.
- 4 C. Combellas, H. Gautier, J. Simon, A. Thiebault, F. Tournilhac, M. Barzoukas, D. Josse, I. Ledoux, C. Amatore and J. Verpeaux, *J. Chem. Soc., Chem. Commun.*, (1988) 203.
- 5 J.C. Kotz, W. Vining, W. Cocco, R. Rosen, A.R. Dias and M. Helena Garcia, *Organometallics*, 2 (1983) 68.
- 6 M.J. Calhorda, M.A.A.F. de C.T. Carrondo, A.R. Dias, A.M.T. Domingos, M.T.L.S. Duarte, M.H. Garcia and C.C. Rom o, *J. Organomet. Chem.*, 320 (1987) 63.
- 7 W.J. Geary, *Coord. Chem. Rev.*, 7 (1977) 81.
- 8 F.H. Allen, O. Kennard and R. Taylor, *Acc. Chem. Res.*, 16 (1983) 146.
- 9 T.C. Wright, G. Wilkinson, M. Motevalli and M.B. Hursthouse, *J. Chem. Soc., Dalton Trans.*, (1986) 2017.
- 10 P. Jernakoff, G.L. Geoffroy, A.L. Rheingold and S.J. Geib, *J. Chem. Soc., Chem. Commun.*, (1987) 1610.
- 11 M.A.A.F. de C.T. Carrondo, A.R. Dias, M.H. Garcia, A. Mirpuri, M.F.M. Piedade and M.S. Salema, *Polyhedron*, 8 (1989) 2439.
- 12 G.J. Kubas and R.R. Ryan, *Inorg. Chem.*, 23 (1984) 3181.
- 13 M.A.A.F. de C.T. Carrondo, P.M. Matias and G.A. Jeffrey, *Acta Crystallogr., Sect. C*, 40 (1984) 932.
- 14 H. Werner, B. Ulrich, U. Schubert, P. Hofmann and B. Zimmer-Gasser, *J. Organomet. Chem.*, 297 (1985) 27.
- 15 M.M. Kubicki, R. Kergoat, L.C. Gomes de Lima, M. Cariou, H. Scordia, J.E. Guerchais and P. L'Haridon, *Inorg. Chim. Acta*, 104 (1985) 191.

- 16 F. Conan, J.-E. Geurchais, R. Mercier, J. Sala-Pala and L. Toupet, *J. Chem. Soc., Chem Commun.*, (1988) 345.
- 17 M.J. Calhorda, M.A.A.F. de C.T. Carrondo, M.H. Garcia and M.B. Hursthouse, *J. Organomet. Chem.*, 342 (1988) 209.
- 18 M.J. Calhorda, M.A.A.F. de C.T. Carrondo, A.R. Dias, C.F. Frazão, M.B. Hursthouse, J.A.M. Simões and C. Teixeira, *Inorg. Chem.*, 27 (1988) 2513.
- 19 M.J. Calhorda, M.A.A.F. de C.T. Carrondo, R. Gomes da Costa, A.R. Dias, M.T.L.S. Duarte and M.B. Hursthouse, *J. Organomet. Chem.*, 320 (1987) 53.
- 20 K. Prout, T.S. Cameron, R.A. Forder, S.R. Critchley, B. Denton, G.V. Rees, *Acta Crystallogr., Sect. B*, 30 (1974) 2290.
- 21 M.J. Calhorda, M.A.A.F. de C.T. Carrondo, A.R. Dias, A.M.T.S. Domingos, J.A.M. Simões and C. Teixeira, *Organometallics*, 5 (1986) 660.
- 22 J.W. Layer and R. Hoffmann, *J. Am. Chem. Soc.*, 98 (1976) 1729.
- 23 S.K. Kurtz and T.T. Perry, *J. Appl. Phys.*, 39 (1968) 3798.
- 24 M.L.H. Green and P.J. Knowles, *J. Chem. Soc., Perkin Trans.*, (1973) 989.
- 25 R.L. Cooper and M.L.H. Green, *J. Chem. Soc. (A)*, (1967) 1155.
- 26 M.L.H. Green and W.E. Lindsell, *J. Chem. Soc. (A)*, 1(1967) 1455.
- 27 I.V. Nelson and R.T. Iwamoto, *Anal. Chem.*, 35 (1963) 867.
- 28 N. Walker and D. Stuart, *Acta Crystallogr., Sect. A*, 39 (1983) 158.
- 29 G.M. Sheldrick, in G.M. Sheldrick, C. Kruger and R. Goddard (Eds.), *Crystallographic Computing 3*, Oxford University Press, 1985, pp. 175-189.
- 30 G.M. Sheldrick, *SHELX Crystallographic Calculation Program*, University of Cambridge, 1976.
- 31 J.-O. Lundgren, *UPALS-A Full-matrix Least-Squares Refinement Program*, Institute of Chemistry, Uppsala, 1978.
- 32 C.K. Johnson, *ORTEP-II*, Report ORNL-5138, Oak Ridge National Laboratory, Oak Ridge, Tennessee, 1976.
- 33 *International Tables for X-Ray Crystallography*, Vol. IV, Kynoch Press, Birmingham, England, 1974.